

Spin quantum Hall effect and plateau transitions in multilayer network models

J. T. Chalker

Theoretical Physics, Oxford University, 1, Keble Road, Oxford, OX1 3NP, United Kingdom

M. Ortuño and A. M. Somoza

Departamento de Física—CIOyN, Universidad de Murcia, Murcia 30.071, Spain

(Received 30 November 2010; published 15 March 2011)

We study the spin quantum Hall effect and transitions between Hall plateaus in quasi-two-dimensional network models consisting of several coupled layers. Systems exhibiting the spin quantum Hall effect belong to class C in the symmetry classification for Anderson localization, and for network models in this class there is an established mapping between the quantum problem and a classical one involving random walks. This mapping permits numerical studies of plateau transitions in much larger samples than for other symmetry classes, and we use it to examine localization in systems consisting of n weakly coupled layers. Standard scaling ideas lead one to expect n distinct plateau transitions, but in the case of the unitary symmetry class this conclusion has been questioned. Focusing on a two-layer model, we demonstrate that there are two separate plateau transitions, with the same critical properties as in a single-layer model, even for very weak interlayer coupling.

DOI: [10.1103/PhysRevB.83.115317](https://doi.org/10.1103/PhysRevB.83.115317)

PACS number(s): 72.15.Rn, 64.60.De, 05.40.Fb

I. INTRODUCTION

Universality classes for critical behavior at Anderson transitions are determined by the dimensionality and the symmetries of the Hamiltonian.¹ The best-known universality classes are the three Wigner-Dyson classes originally identified in the context of random matrix theory. Seven additional symmetry classes for localization were recognized² over a decade ago: they are distinguished from the Wigner-Dyson classes by having a special point in the energy spectrum and energy levels that appear in pairs either side of this point. In one of these additional classes, known as class C, properties of suitably chosen quantum lattice models can be expressed in terms of observables for a classical model defined on the same lattice. This mapping was originally discovered³ in the context of the spin quantum Hall effect (SQHE), where it relates a delocalization transition in two dimensions to classical percolation, also in two dimensions, for which many relevant aspects of critical behavior are known exactly.

Models in class C arise from the Bogoliubov–de Gennes Hamiltonian for quasiparticles in a gapless, disordered spin-singlet superconductor with broken time-reversal symmetry for orbital motion but negligible Zeeman splitting. The special energy in this case is the chemical potential (which we set to zero) and pairs of levels are related by particle-hole symmetry, which has profound consequences for the influence of disorder on quasiparticle eigenstates. The quantum-to-classical mapping provides a framework within which quasiparticle properties can be studied in great detail starting from a simplified description of a disordered superconductor.

Here we use this approach to study for the SQHE an aspect of the plateau transition that has resisted detailed investigation in the context of the conventional integer quantum Hall effect (IQHE) belonging to the unitary symmetry class. Specifically, we study plateau transitions in models of n weakly coupled layers. For such systems, scaling ideas⁴ and the σ model description⁵ lead one to expect n distinct transitions, separating adjacent pairs of phases in which the Hall conductance differs by one quantum unit, irrespective of how weakly the layers

are coupled. The same scaling ideas have other important consequences. In particular, they suggest a scenario for the disappearance of the IQHE as magnetic field strength is reduced, in which extended states responsible for plateau transitions levitate^{6,7} in energy, and they are input for construction of the global phase diagram,⁸ in which the Hall conductance of adjacent IQHE phases again differs by one quantum unit. Alternative types of behavior have also been proposed, involving direct transitions between phases with Hall conductance differing by multiple quantum units,⁹ and there has developed quite an extensive literature on the subject, reviewed in Ref. 10. Attempts^{11–16} to distinguish between these different possibilities using numerical simulations are hampered by the fact that in the most interesting regimes—weak magnetic field or weak interlayer coupling—the localization length is never short, making asymptotic behavior hard to reach. Even in one of the simplest settings, involving a two-layer IQHE system as a representation of a spin-degenerate Landau level, the existence of two transitions has been inferred only rather indirectly. By contrast, we show in the following for the SQHE that the mapping to a classical description allows simulation of sufficiently large systems that the behavior expected from scaling and the σ model can be revealed in considerable detail.

The mapping³ between a single-layer network model for the SQHE and classical percolation generalizes to all models in the same symmetry class that share a set of key features.¹⁷ A variety of physical quantities of interest for localization (although not all) can be determined in this way, including the two-terminal conductance of a finite sample, which will be our main tool. The generalization, however, relates the quantum problem to a classical one involving interacting random walks rather than percolation, so that while much is known analytically about percolation, simulations are required to study properties of the classical walks. Since these classical simulations are much less computationally intensive than a direct study of the quantum problem, much larger system sizes are accessible. Here we exploit the classical mapping to study the conductance of quasi-two-dimensional SQHE systems.

Similar conclusions to the ones we present have been suggested in earlier work,¹⁹ but from a much more restricted range of system sizes. Our results for quasi-two-dimensional systems are complementary to recent work on the metal-insulator transition in a three-dimensional class C network model, in which the classical mapping enabled a measurement of critical exponents with a precision unprecedented for a localization transition.¹⁸

While our focus is on properties of the quantum system, we believe that the classical walks we study deserve attention in their own right. In particular, it would be interesting if arguments could be found directly for the classical problem, to show that the n -layer system has n transitions, and that these are in the same universality class as classical percolation on the plane.

II. MODEL

We study models in which quasiparticles propagate along the directed links of a lattice and scatter between links at nodes. Disorder enters the models in the form of quenched random phase shifts associated with propagation on links. For class C models, the disorder-averaged (spin) conductance can be expressed as an average over configurations of interacting classical random walks on the same directed lattice.^{3,17} This relation between quantum properties and classical walks holds on any graph in which all nodes have exactly two incoming and two outgoing links. In the classical problem the connection at each node is a quenched random variable having two possible arrangements. Incoming and outgoing links are arranged in pairs, and a particle passing through the node follows the pairing with probability p , or switches with probability $1 - p$. Given a directed graph with the required coordination, any choice of classical connections at the nodes separates paths on the graph into a set of distinct, closed, mutually avoiding walks. Average properties of these walks are calculated from a sum over all node configurations, weighted according to their probabilities.

Here we consider systems formed from several coupled layers. Each layer is an $L \times L$ square sample of the L lattice, shown schematically in Fig. 1. It is characterized by the node probability p and in isolation has a plateau transition at $p = 1/2$. We construct n -layer models by stacking n copies of this lattice in register, with independent disorder realizations in each layer. For $n = 2$ we couple the layers using a second set of nodes, located at the midpoints of the links in each layer. This set of nodes is characterized by the probability p_1 of switching layers, and the model is symmetric under $p_1 \rightarrow 1 - p_1$. At $p_1 = 0$, and also at $p_1 = 1$, the system separates into independent layers, both with a plateau transition at $p = 1/2$; we are concerned with behavior as a function of p for $0 < p_1 < 1$, and in particular whether two coupled layers exhibit two transitions at separate values of p . We also examine, though in less detail, a three-layer system, considering only a parameterless form of interlayer coupling. This is constructed by allowing at the midpoints of the links in each layer all six permutations of trajectories between layers, with equal probability.

We calculate the two-terminal conductance between opposite, open faces as the average number of classical trajectories

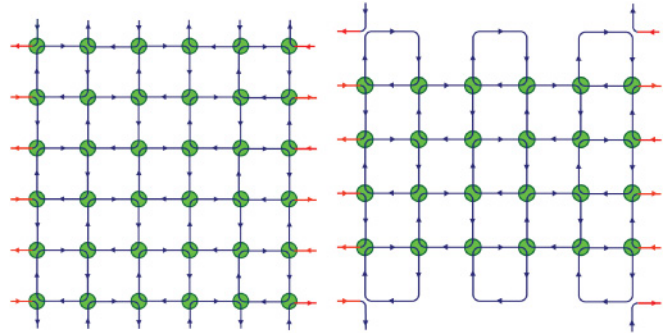


FIG. 1. (Color online) The L lattice: circles represent nodes at which links are connected as indicated with probability p , and in the opposite sense with probability $1 - p$. Left and right panels indicate the boundary conditions applied to obtain the quantities we refer to respectively as the longitudinal conductance and Hall conductance. In both cases, current leads are attached to the left and right edges. For calculation of the longitudinal conductance, periodic boundary conditions are applied to the top and bottom edges to form a cylinder. For the Hall conductance, reflecting boundary conditions are applied to the top and bottom edges.

connecting these two faces. We use two different types of boundary condition in the other direction, as illustrated in Fig. 1. With periodic boundary conditions, so that the sample is a cylinder, the two-terminal conductance of a system described by a constant local conductivity tensor would be simply the longitudinal conductivity. For that reason we call the average conductance in this geometry the *longitudinal conductance*. Alternatively, using reflecting boundary conditions, the two-terminal conductance within a Hall plateau is determined by the number of edge states. We therefore call the average conductance in this geometry the *Hall conductance*, even though its value between Hall plateaus depends on both components of the conductivity tensor. Within the framework of the quantum-to-classical mapping we use, the disorder-averaged spin conductance $G(p, L)$ of the quantum system is given (in units of $\hbar/4\pi$) by the average of the number of classical paths from a specified open face to the other.

Our simulations use system sizes L of between 500 and 5000 lattice spacings. For the largest system, we average up to 10^6 disorder realizations. Earlier work¹⁹ was limited to $L \leq 80$.

III. CONDUCTANCE AND SPIN QUANTUM HALL TRANSITIONS

We first study the two-layer system at interlayer coupling $p_1 = 1/2$. In Fig. 2 we show the behavior of the longitudinal and transverse conductances as functions of the intralayer parameter p for two system sizes. Two transitions are apparent, at $p \simeq 0.43$ and $p \simeq 0.57$, separating three phases characterized by quantized Hall conductances of 0, 1, and 2 units. The accurate quantization of the Hall conductance in the central phase is striking. In terms of classical walks, it arises because almost all realizations that contribute to the average have exactly one extended trajectory at each reflecting edge. Other trajectories in this phase are typically much shorter than

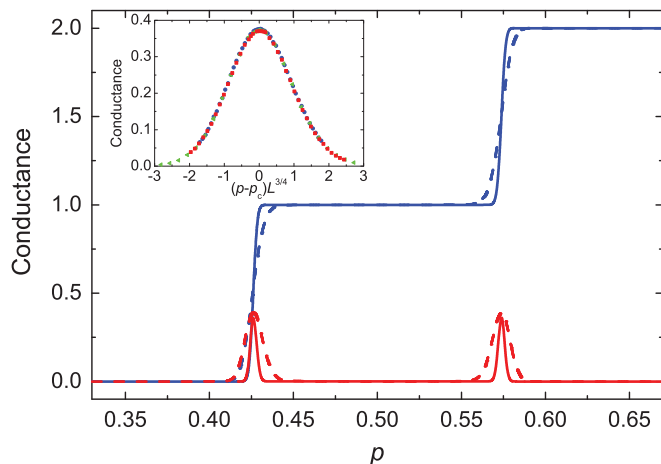


FIG. 2. (Color online) Conductance of the two-layer system at $p_1 = 1/2$ as a function of p for system sizes $L = 1000$ (dashed lines) and 4000 (continuous lines). Curves with steps (blue) represent the Hall conductance, obtained with reflecting boundary conditions. Curves with peaks (red) are the longitudinal conductance, obtained with a cylindrical sample. The inset shows the scaling of the longitudinal conductance near the first peak as a function of $(p - p_c)L^{3/4}$ for $L = 3000, 4000$, and 5000 .

the sample size, since the longitudinal conductance is very small.

These transitions in the two-layer system are expected to have the same critical behavior as for a single layer, which maps to that of the percolation transition. As a first test, we plot in the inset to Fig. 1 the longitudinal conductance near the peak at $p \simeq 0.43$ as a function of $(p - p_c)L^{3/4}$ for three system sizes $L = 3000$ (blue dots), 4000 (green triangles), and 5000 (red squares). The good overlap of the data for different sizes shows that the widths of the peaks in longitudinal conductance scale as $L^{-1/\nu}$, where $\nu = 4/3$ is the correlation length exponent for percolation. The width of the steps in Hall conductance follows a similar behavior.

As a second and more precise check of universality, we examine the peak value of the longitudinal conductance. In a single layer this can be deduced from the crossing probabilities for percolation clusters in an annulus.^{3,20} We obtain values for these from Ref. 21: the probability of a single crossing in a square sample with cylindrical boundary conditions is $0.357369\dots$ and the probability of two crossings is $0.002018\dots$, while higher-order crossings are negligible at our precision. So the exact value of the critical conductance in this geometry from percolation theory is $0.361404\dots$. To test our numerical approach, we first calculate the maximum value of the longitudinal conductance for a single layer using a sequence of system sizes at the exact critical probability for percolation, $p = 1/2$. We find that deviations of these maxima from the large-system limit decrease roughly proportionally to L^{-1} , so we extrapolate to infinite size by plotting maxima as a function of L^{-1} . We show the result in Fig. 3. A linear fit yields the intercept 0.36135 ± 0.00010 , confirming the reliability of the approach. We also obtain the maximum conductance for a bilayer system, but this time we do not know the exact critical probability for percolation so we have to calculate the conductance for several probabilities in the critical region and

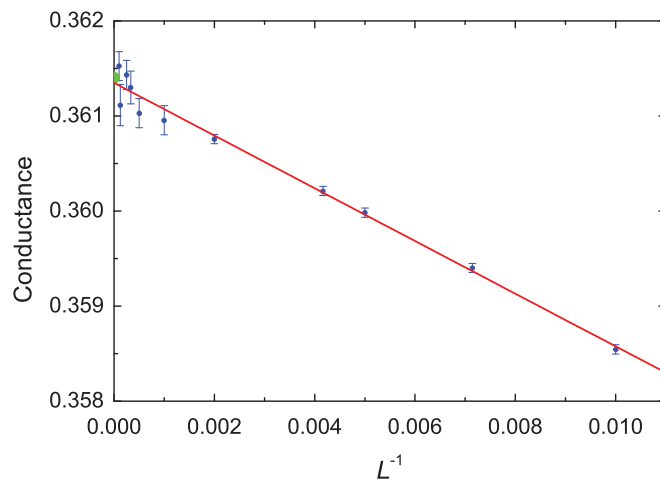


FIG. 3. (Color online) Conductance of a single-layer system at criticality, $p = 1/2$, versus L^{-1} . The large dot on the vertical axis corresponds to the exact value.

fit the results with a Gaussian to extract the maximum value at each system size. The deviations of this maximum value from the large-system limit do not scale as either L^{-1} or $L^{-3/4}$ for the range of system sizes considered. To extract a limiting value of the critical conductance for the bilayer system, we therefore first plot the difference between the bilayer maximum conductances and the critical conductance given by percolation theory, as a function of L on a double-logarithmic scale. The result is shown in the inset to Fig. 4: the data lie close to a straight line with slope $x = 0.662$. We then plot in the main part of Fig. 4 the conductance as a function of L^{-x} . This figure shows that the conductance extrapolates to a value close to the one from percolation theory, and we obtain 0.3613 ± 0.0002 . The uncertainty is higher than for a single layer because the critical value of p is not known exactly and because the system sizes employed are necessarily smaller.

We have also studied the conductance for the three-layer model described above. Results are shown in Fig. 5. As

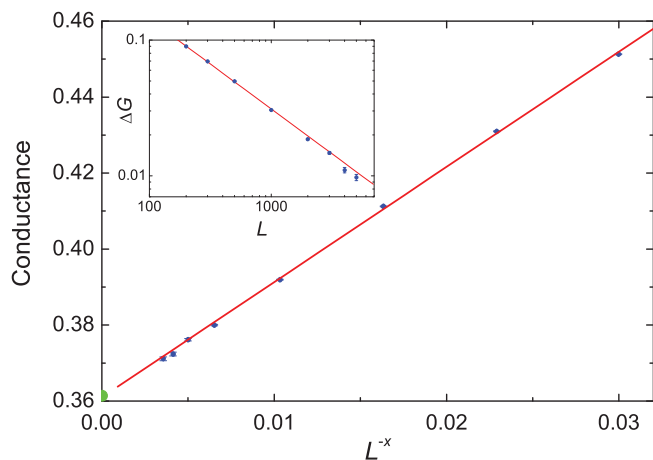


FIG. 4. (Color online) Maximum value of the conductance of a two-layer system as a function of $L^{-0.662}$. The large dot on the vertical axis corresponds to the exact value for percolation. Inset: maximum conductance, with respect to the percolation value, versus L on a double-logarithmic scale.

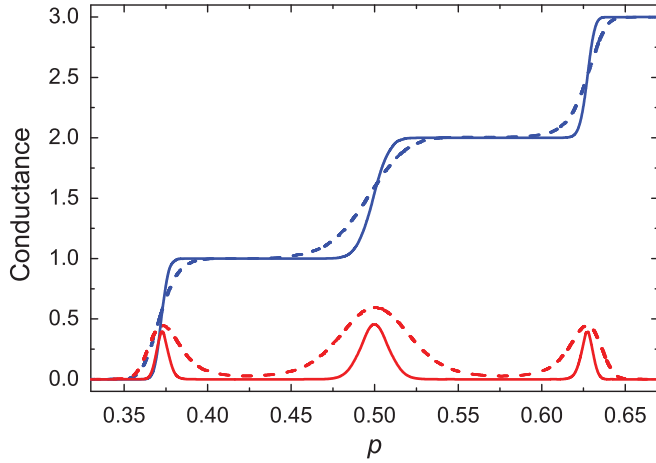


FIG. 5. (Color online) Conductance as a function of p for the three-layer system defined in the text, with system sizes $L = 1000$ (dashed lines) and 4000 (continuous lines). Curves with steps (blue) represent the Hall conductance, obtained with reflecting boundary conditions. Curves with peaks (red) are the longitudinal conductance, obtained with a cylindrical sample.

expected, three distinct transitions separate four phases, and adjacent phases have Hall conductances differing by a single unit; the critical points are at $p \simeq 0.37, 0.5, \text{ and } 0.63$.

IV. PHASE DIAGRAM FOR A TWO-LAYER SYSTEM

The results presented in the previous section are for maximal coupling between layers, and it is interesting to examine how behavior changes as this coupling is reduced. In particular, a key question is whether the degenerate transition occurring at $p = 1/2$ for n uncoupled layers is split into n distinct transitions by any nonzero interlayer coupling, or whether a step in Hall conductance of more than one unit persists for small couplings. We focus on properties of the two-layer system as a function of the interlayer coupling p_1 , and calculate the longitudinal conductance rather than Hall conductance because it is easier to locate the transition probabilities using this quantity. For all system sizes and values of p_1 at which there are two clear peaks in the longitudinal conductance as a function of p , we determine peak positions p_c by fitting the conductance of one of them to a Gaussian in $p - p_c$. At each value of p_1 we make an extrapolation of these peak positions to infinite system size, linearly in $L^{-\alpha}$. We find empirically that $\alpha = 2$ is the best fitting exponent in all cases considered, but the results do not depend much on this value. We consider sizes L from 500 to 5000. In large systems it is possible to identify two distinct transitions even at very weak interlayer coupling. For example, with $p_1 = 5 \times 10^{-4}$ we can distinguish two peaks for sizes greater than 1000, and for $p_1 = 10^{-3}$ we can discriminate for sizes greater than 500. The extrapolated values of the critical probability for the transitions are shown in Fig. 6.

To gain further insight, we analyze in detail the shape of the phase boundary at small interlayer coupling. In this regime p_c is close to $1/2$ and if two distinct transitions persist for all nonzero p_1 , we expect a relation of the form

$$p_1 \propto |p_c - 1/2|^\gamma. \quad (1)$$

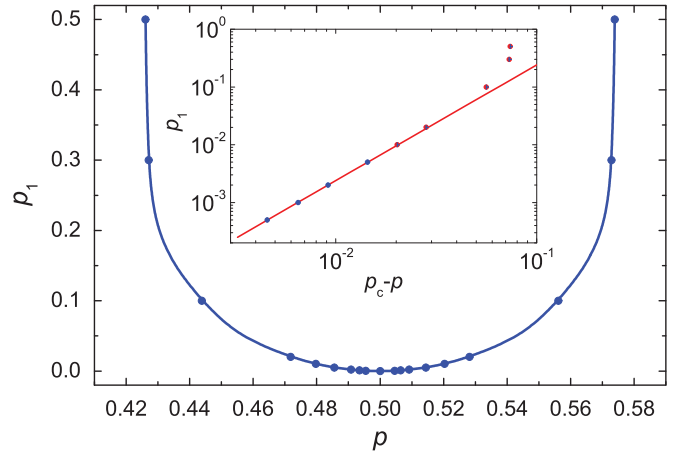


FIG. 6. (Color online) Phase boundaries for spin quantum Hall states in a two-layer system, as a function of the intralayer parameter p and the interlayer parameter p_1 . Points are from extrapolations described in the main text; the continuous curve is a guide to the eye. Inset: same data on a double-logarithmic scale.

In the inset to Fig. 4 we show p_1 versus $p_c - 1/2$, on a double-logarithmic scale. The straight line is a linear fit to the four points with smallest p_1 . Its slope is $\gamma = 2.004 \pm 0.002$. The fact that the phase boundary is accurately described by Eq. (1) is good evidence for the correctness of the quantum Hall scaling flow diagram of Ref. 4 when applied to the SQHE. It is also evidence that in the system studied there is no direct transition between phases with Hall conductance differing by more than one unit.

The value $\gamma = 2$ can be understood by the following argument. Consider first a single-layer system, and let $\xi(p)$ be the correlation length for classical walks: the typical diameter of the largest closed loops. These loops are the hulls of percolation clusters, and for large $\xi(p)$ their arclength varies as $\xi(p)^{d_h}$ with $d_h = 7/4$. Moreover, from the mapping³ for a single layer to classical percolation, we know that $\xi(p)$ diverges as $\xi(p) \propto |p - 1/2|^{-\nu}$ with $\nu = 4/3$ when p approaches $1/2$. Next examine the probability in a two-layer system that a pair of such loops, one from each layer, are coupled. This probability is expected to be of order 1 for $p = p_c$. It is made up of the product of three factors: the length $\xi(p)^{d_h}$ of one loop, the density $\xi(p)^{d_h-2}$ of the other loop, and the probability p_1 that a given pair of links in equivalent positions in the two layers are coupled. We therefore expect $p_1 \propto \xi(p_c)^{2-2d_h}$ and hence $p_1 \propto |p - 1/2|^{2\nu(d_h-1)} = |p - 1/2|^2$. It is interesting to note the difference between this result for the SQHE and the equivalent one for a two-layer IQHE system, in which²² (taking over the notation we have defined for the SQHE) $p_1 \propto |p_c - 1/2|^\nu$. In the language of the quantum localization problem, this difference arises because the density of states vanishes at the mobility edge for the SQHE but is finite for the IQHE.

ACKNOWLEDGMENTS

This work was supported by EPSRC Grant No. EP/D050952/1, by DGI Grant No. FIS2009-13483, and by Fundacion Seneca, Grant No. 08832/PI/08.

- ¹F. Evers and A. D. Mirlin, *Rev. Mod. Phys.* **80**, 1355 (2008).
- ²A. Altland and M. R. Zirnbauer, *Phys. Rev. B* **55**, 1142 (1997); M. R. Zirnbauer, *J. Math. Phys.* **37**, 4986 (1996).
- ³I. A. Gruzberg, A. W. W. Ludwig, and N. Read, *Phys. Rev. Lett.* **82**, 4524 (1999).
- ⁴D. E. Khmel'nitzkii, *Pis'ma Zh. Eksp. Teor. Fiz.* **38**, 454 (1983) [*JETP* **38**, 552 (1983)].
- ⁵H. Levine, S. B. Libby, and A. M. M. Pruisken, *Phys. Rev. Lett.* **51**, 1915 (1983).
- ⁶D. E. Khmel'nitzkii, *Phys. Lett. A* **106**, 182 (1984).
- ⁷R. B. Laughlin, *Phys. Rev. Lett.* **52**, 2304 (1984).
- ⁸S. Kivelson, D.-H. Lee, and S.-C. Zhang, *Phys. Rev. B* **46**, 2223 (1992).
- ⁹G. Xiong, S.-D. Wang, Q. Niu, D.-C. Tian, and X. R. Wang, *Phys. Rev. Lett.* **87**, 216802 (2001); D. Z. Liu, X. C. Xie, and Q. Niu, *ibid.* **76**, 975 (1996); D. N. Sheng and Z. Y. Weng, *ibid.* **78**, 318 (1997).
- ¹⁰V. V. Mkhitarian, V. Kagalovsky, and M. E. Raikh, *Phys. Rev. B* **81**, 165426 (2010).
- ¹¹D. K. K. Lee and J. T. Chalker, *Phys. Rev. Lett.* **72**, 1510 (1994).
- ¹²Z. Wang, D.-H. Lee, and X.-G. Wen, *Phys. Rev. Lett.* **72**, 2454 (1994).
- ¹³C. B. Hanna, D. P. Arovas, K. Mullen, and S. M. Girvin, *Phys. Rev. B* **52**, 5221 (1995).
- ¹⁴V. Kagalovsky, B. Horovitz, and Y. Avishai, *Phys. Rev. B* **52**, 17044 (1995).
- ¹⁵E. S. Sorensen and A. H. MacDonald, *Phys. Rev. B* **54**, 10675 (1996).
- ¹⁶X. Wan and R. N. Bhatt, *Phys. Rev. B* **64**, 201313 (2001).
- ¹⁷E. J. Beamond, J. Cardy, and J. T. Chalker, *Phys. Rev. B* **65**, 214301 (2002).
- ¹⁸M. Ortuño, A. M. Somoza, and J. T. Chalker, *Phys. Rev. Lett.* **102**, 070603 (2009).
- ¹⁹E. J. Beamond, D.Phil. thesis, Oxford University, 2002.
- ²⁰J. L. Cardy, *Phys. Rev. Lett.* **84**, 3507 (2000).
- ²¹J. L. Cardy, *J. Phys. A* **35**, L565 (2002).
- ²²J. T. Chalker and A. Dohmen, *Phys. Rev. Lett.* **75**, 4496 (1995).